Mixed Thioether/Amine-Functionalized Expanded Calixarenes, Related Macropolycycles, and Metal Complexes thereof

Josef Taut, Frederik Schleife, Martin Börner, Clément Bonnot, Henri-Pierre Jacquot de Rouville, Jean-Claude Chambron, Berthold Kersting

EurJIC
European Journal of Inorganic Chemistry

Research Article
doi.org/10.1002/ejic.202300580

Chemistry Europe
European Chemical Societies Publishing

www.eurjic.org

Mixed Thioether/Amine-Functionalized Expanded Calixarenes, Related Macropolycycles, and Metal Complexes thereof

Josef Taut,[a, b] Frederik Schleife,[a] Martin Börner,[a] Clément Bonnot,[c] Henri-Pierre Jacquot de Rouville,[b] Jean-Claude Chambron,*[b, c] and Berthold Kersting*[a]

A series of tetraaza-expanded calix[4]arene analogues (**2**–**4**), in which two of the four aryl groups are ethylene-protected thiophenol components were prepared from tetraaldehyde **1**. Two of these strapped macrocycles were characterized crystallographically, as well as the dipalladium complex of **4**. The same tetraaldehyde had been previously used for the synthesis of a macrotricycle (**5**) and a macropentacycle (**6**), the coordination properties of which have been investigated. In particular, ligand **6** was shown to be able to encapsulate a Cu^{+} or a Ag^{+} ion in the tetrahedral coordination pocket offered by a bridgehead nitrogen atom and the three proximal thioether sulfur atoms.

Introduction

The metal binding sites of metalloproteins involve amino-acid residues that play the role of neutral or anionic ligands, such as the histidine imidazole for nitrogen and the cysteine thiolate for sulfur. Oxygen-based ligands, *i.e.* phenolate and carboxylate, derive from a greater variety of aminoacids, such as tyrosine on the one hand, aspartate and glutamate on the other hand.[1] Among sulfur containing ligands, the anionic cysteine thiolate is probably more frequently encountered in the active site of metalloproteins than the neutral methionine thioether.[2] Methionine is however involved in the coordination of the metal centers of electron transfer metalloenzymes, such as Cu in azurin and plastocyanin, and Fe(II) in cytochrome c,[3] and the Cu(I) transport protein Ctr1,[4] just to mention a few. Methionine is also found in the ubiquitous natural resistance-associated macrophage protein (Nramp) family of metal transporters,[5] which are able to bind biologically-important metal cations in the +2 oxidation state such as Mn^{2+}, Fe^{2+}, Co^{2+}, Ni^{2+}, Cu^{2+} and Zn^{2+}, and discriminate them against the more abundant divalent alkaline earth metal cations Mg^{2+} and Ca^{2+}. For example, in ScaNramp (Nramp of *Staphylococcus capitis*) the metal cation is surrounded by one sulfur and three oxygen atoms. It is precisely the soft sulfur atom of the methionine residue that is responsible for the discrimination between cations of group IIA and biologically-relevant first row transition and related divalent metal cations.[6] However, methionine is more frequently associated with nitrogen ligands, such as the heme in cytochrome c or imidazole in azurin. In the past, ligands combining nitrogen donor atoms and thioether sulfur donor atoms belonged to the aza crownthioether family, and were used for the preparation of binuclear Cu(I) complexes.[7] More recently, NTA-based tripod ligands incorporating methionine pendants were used as Ctr1 mimics,[8] and a piperazine substituted by methylthioether and thiolate arms formed a Ni(II) complex trimer that showed ACS-like reactivity.[9]

We have been interested for several years in macrocycles obtained by expansion of the tetramercaptocalix[4]arene platform by insertion of bis(methylene)aza- or longer nitrogen-containing bridges between the thiophenol functions.[10] These compounds were prepared through intermediates in which the thiophenol functions are protected in thioether form. In particular, starting from an ethylene-bridged arylthioether proved very useful as it played the role of an organic template. It was cleaved in the end of the synthesis, releasing the thiolate functions, which were subsequently involved in metal cation complexation. In this work, we investigate the overlooked coordination chemistry of thioether intermediates of the expanded azacalix[4]arenes, as well as related macropolycycles exhibiting a diversity of topologies. Noteworthy, all the compounds of Figure 1 derive from tetraaldehyde **1**,[11] *i.e.* macrobicycles **2**–**4**, macrotricyclic **5**, and macropentacycle **6**.[12] We report here the synthesis of compounds **2**–**4**, the complexation of Pd^{2+} by **3**, and the complexation of **6** by Cu^{+} and Ag^{+}.

[a] *J. Taut, Dr. F. Schleife, Dr. M. Börner, Prof. Dr. B. Kersting*
Institut für Anorganische Chemie
Universität Leipzig
Johannisallee 29, 04103 Leipzig (Germany)
E-mail: b.kersting@uni-leipzig.de

[b] *J. Taut, Dr. H.-P. Jacquot de Rouville, Dr. J.-C. Chambron*
Institut de Chimie de Strasbourg (UMR 7177)
Université de Strasbourg and the CNRS
4, rue Blaise Pascal, 67070 Strasbourg (France)
E-mail: jcchambron@unistra.fr

[c] *Dr. C. Bonnot, Dr. J.-C. Chambron*
Institut de Chimie Moléculaire de l'Université de Bourgogne (UMR 6302)
Université de Strasbourg and the CNRS
9, avenue Alain Savary, 21078 Dijon (France)

Supporting information for this article is available on the WWW under https://doi.org/10.1002/ejic.202300580

Research Article
doi.org/10.1002/ejic.202300580

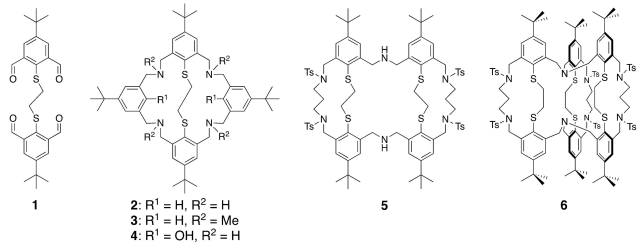

Figure 1. The tetraaldehyde precursor (**1**) and the macropolycyclic ligands (**2**–**6**) synthesized therefrom.

Results and Discussion

Synthesis and characterization of ligands

The ethylene-bridged thiacalix[4]arenes **2** and **3** were prepared according to a two-step procedure as illustrated in Scheme 1. Thus, condensation reaction involving the tetraaldehyde **1** and 1,3-bis(aminomethyl)benzene under high-dilution conditions, followed by $NaBH_4$ reduction of the intermediate tetra-imine furnished the bicyclic amino-thioether **2** in 91% yield. The high yield can be traced to the high dilutions employed, and also to the template effect played by the ethylenic linkage in the tetraaldehyde **1**. The linkage brings the four aldehyde functions in close proximity, such that the cyclization reaction is favored over the polymerization reactions. Some preorganization within the bis(aminomethyl)benzene most likely is also a factor that contributes to the high yield of the cyclization reaction. The protection of the thiolate functions in **2** is an attractive feature, and allows functionalization of the secondary amine functions. Thus, the Eschweiler–Clarke reaction of **2** with formic acid and formaldehyde provided the permethylated macrocycle **3** in high yield without affecting the masked thiolate functions.

For the preparation of tetraamine thioether **10** (Scheme 2), the first step was to reduce the four aldehyde functions of **1** using sodium borohydride in an ethanol/dichloromethane mixture, which gave derivative **7** in very good yield. To introduce nitrogen functions, this compound was converted to tetraazide **9**. This process can be achieved in two different ways (Scheme 2). One possibility (method A) is a substitution in Mitsunobu conditions.[13] Accordingly, **7** was reacted with triphenylphosphine, diisopropylazodicarboxylate, and diphenylphosphoryl azide as the azide source. After purification by column chromatography, tetraazide **9** was obtained in a moderate yield (35%). In order to obtain the tetraazide in better yield and in larger amounts, the classical two-step route involving the mesylate intermediate was chosen (method B). For this purpose, **7** was reacted with mesyl chloride in the presence of triethylamine, which afforded the tetramesylate **8** in 96% yield. This intermediate was subsequently reacted with the stoichiometric amount of sodium azide, which afforded the tetraazide derivative **9** in the form of colorless oil in very good yields without purification. Comparing the two synthetic routes for the preparation of **9**, it is clear that method B is favored. The yield of 93% over the two steps was clearly higher than the yield of only 35% achieved by the Mitsunobu reaction. Another advantage of method B over method A is that complex column-chromatographic purification is not necessary, which simplifies the preparation of larger amounts of compound **9**. The azide functions of **9** were then reduced to amine by catalytic hydrogenation, affording the tetramine derivative **10** in 90% yield.

To prepare macrobicyclic thioether **4**, **10** was reacted with 4-*tert*-butyl-2,6-diformylphenol in a macrocyclization reaction under high dilution conditions, followed by in situ selective reduction of the imine functions with $NaBH_3CN$.[14] The product was isolated by precipitation of its hydrochloric salt **10**·4HCl, and obtained in 13% yield after recrystallisation (Scheme 3). This low yield by comparison with the 91% yield of **3** could be traced back to the steric hindrance of the hydroxy substituents in **4**.

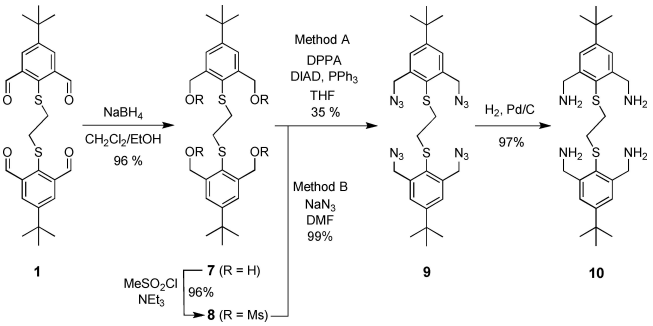

Scheme 2. Synthesis of the tetraamine derivative **10**. DPPA: diphenylphosphoryl azide; DIAD: diisopropylazodicarboxylate; DMF: *N*,*N*-dimethylformamide.

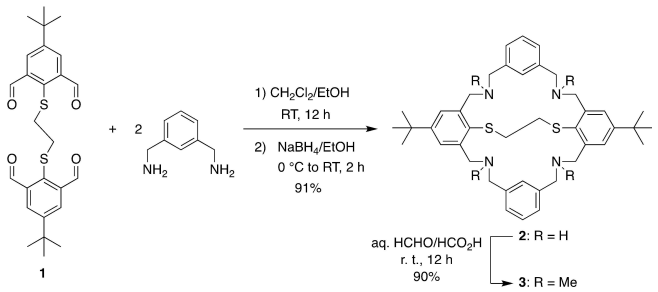

Scheme 1. Synthesis of aza-thioether macrobicycles **2** and **3**.

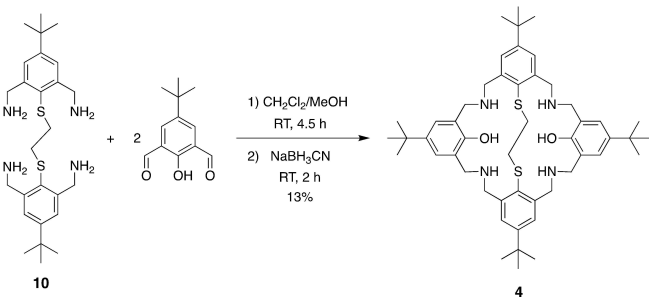

Scheme 3. Preparation of aza-thioether macrobicycle **4**.

Research Article
doi.org/10.1002/ejic.202300580

Crystals of the thioethers **2** and **3** could be grown and were subjected to single-crystal X-ray structure analysis. The molecular structure of **2** is depicted in Figure 2 along with selected bond lengths and angles. The thioether **2** exhibits crystallographically imposed inversion symmetry in agreement with the small number of signals in the ^{1}H NMR spectra. Molecules of **2** are well-separated from each other. Apart from the van der Waals interactions, there are no other intermolecular contacts. In contrast to more flexible amine-thioether macrocycles there are no intramolecular NH···S hydrogen bonding interactions as manifested by the long N···S distances (N1···S1 4.2467(27) Å, N2···S1 4.4923(37) Å). This can be traced to the more rigid 1,3-bis(aminomethyl)-linkers in **2**. The four aryl rings are arranged in an *up*, *up*, *down*, *down* fashion with respect to the plane through the 4 *N* atoms of the macrobicyclic ring. Thus, according to the nomenclature utilized for the parent *p-tert*-butyl-calix[4]arenes, the structure of **2** adopts an 1,2-*alternate* conformation. However, the macrocyclic cavity in **2** is occupied by the ethylene linker, such that no guest inclusion occurs. The C–S sulfur bond lengths are in the normal range for other macrocyclic aryl-alkyl thioethers.[15] Note that the S–CH_2CH_2–S linker in **2** adopts the *anti*-conformation (S–C–C–S dihedral angle = 180°).

Figure 3 displays the molecular structure of the *N*-permethylated derivative **3** of thioether **2**. The thioether is highly twisted, as manifested by the non-coplanarity of the four nitrogen atoms and the saddle-like arrangement of the four aryl rings. To our knowledge, such a twisted structure has not been observed in calix[4]arene chemistry. The twisting in **3** is likely due to the steric demand of the four Me groups installed on the benzylic nitrogen atoms. In contrast to **2**, the S–CH_2CH_2–S linker adopts a *gauche*-conformation with a dihedral angle of 54°. Again the molecules are well-separated from each other. The C–S sulfur bond lengths are very similar to those in **2**.

Complexation properties of 3

Given the high-affinity of the N and S donor atoms for metal ions, we decided to investigate the complexation properties of the macropolycycles. Treatment of **3** with two equiv. of $[PdCl_2(MeCN)_2]$ in acetonitrile at r.t. for 24 h gave a yellow solution, from which an orange-colored solid of composition $[Pd_2Cl_4(\mathbf{3})]$ could be reproducibly isolated in 75% yield (Scheme 4).

The Pd complex was found to be stable in the solid state as well as in solution. The ^{1}H NMR spectrum revealed a singlet for the *tert*-butyl group methyl protons at δ 1.36 and two singlets for the *N*-methyl protons at δ 2.64 and 2.21, indicative of either only one species in solution, or a fast exchange between multiple species. Similarly, the ^{13}C NMR spectrum revealed only one signal for the *tert*-butyl groups methyl carbon atoms. A crystal structure determination of crystals of $[Pd_2Cl_4(\mathbf{3})]\cdot 2.75CH_2Cl_2$ obtained from a CH_2Cl_2/EtOH solution was undertaken to determine the solid state structure. Crystals of $[Pd_2Cl_4(\mathbf{3})]\cdot 2.75CH_2Cl_2$ are orthorhombic, space group P*bca*. The asymmetric unit contains one molecule of a dinuclear mixed-ligand Pd^{2+} complex. Figure 4 provides a perspective view of the structure of the $[Pd_2Cl_4(\mathbf{3})]$ complex and the atomic

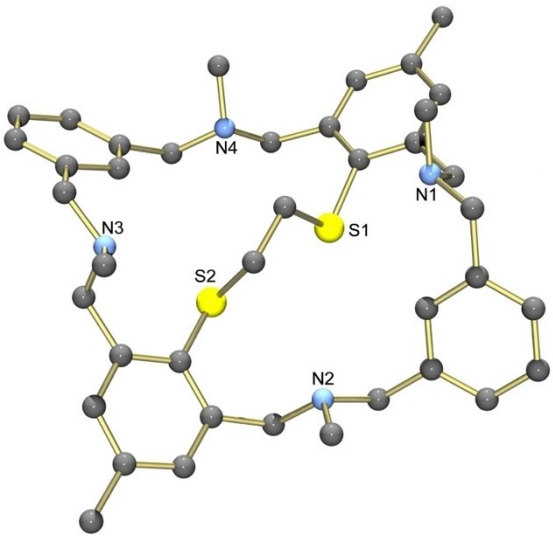

Figure 3. Molecular structure of the permethylated thioether **3**. Hydrogen atoms and methyl groups of the *tert*-butyl substituents have been omitted for clarity. Selected bond lengths/[Å]: S1–C^{Ar} 1.787(2), S1–CH_2 1.8280(19), S2–C^{Ar} 1.788(2), S2–CH_2 1.829(2).

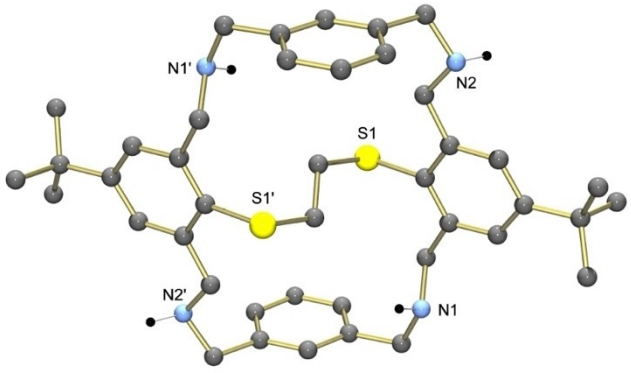

Figure 2. Molecular structure of the thioether **2**. The methyl carbon atoms of the *tert*-butyl groups and the hydrogen atoms, except for NH groups, have been omitted for clarity. S1–C^{Ar} 1.787(3) Å, S1–CH_2 1.817(3) Å. Symmetry codes used to generate equivalent atoms: 1-*x*, 1-*y*, 1-*z* (′).

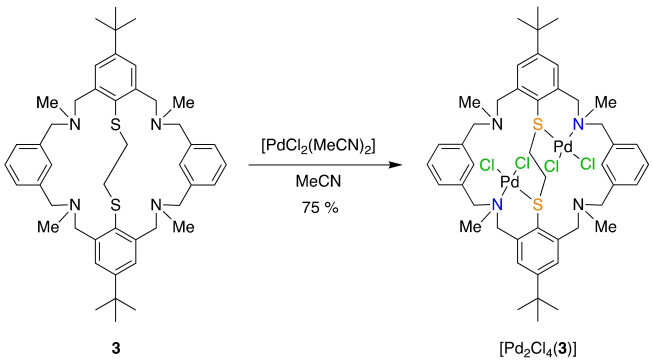

Scheme 4. Preparation of the palladium complex of macrobicycle **3**.

Research Article
doi.org/10.1002/ejic.202300580

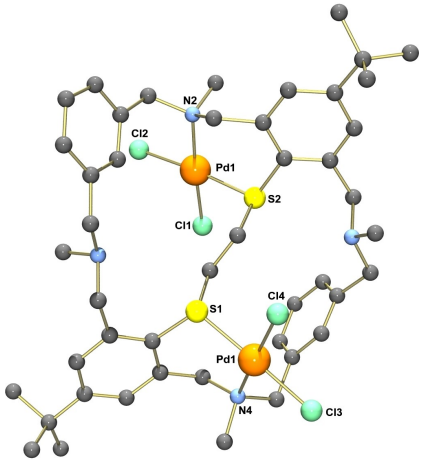

Figure 4. Perspective view of the molecular structure of the $[Pd_2Cl_4(\mathbf{3})]$ complex in the crystal of $[Pd_2Cl_4(\mathbf{3})]\cdot 2.75CH_2Cl_2$. Hydrogen atom and solvate molecules omitted for clarity.

labelling scheme. Table 1 lists selected bond lengths and angles.

The two Pd^{2+} ions in $[Pd_2Cl_4(\mathbf{3})]$ are both four-coordinated being surrounded by one thioether S, one benzylic amine N, and two *cis*-oriented chlorido ligands in a nearly square-planar fashion. The complex was found to be not symmetric contrary to what was suggested by the NMR spectra. The average Pd–S (2.284 Å), Pd–N (2.109 Å), and Pd–Cl (2.316 Å) distances show no unusual features and compare well with those of other four-coordinate Pd^{2+} complexes coordinated by aza-thioether and chlorido ligands.[16] The bond angles about the Pd atoms deviate by as much as 7° from the ideal 90°, most likely due to the constraints of the macrocyclic ligand. In contrast to other expanded calix[4]arenes – which feature a plane through the four benzylic N atoms – there are only three such coplanar N atoms (N1, N3, N4) in the coordinated macrobicycle **3**. The four aromatic rings in $[Pd_2Cl_4(\mathbf{3})]$ are arranged in an *up*, *up*, *down*, *down* fashion with respect to the plane through these three benzylic N atoms. According to the nomenclature utilized for the parent *p-tert*-butyl-calix[4]arenes, the conformation of **3** in $[Pd_2Cl_4(\mathbf{3})]$ can thus be referred to a distorted 1,2-*alternate*-conformer. It is not clear whether this conformation is also present in the liquid phase.

Table 1. Selected bond lengths and angles in $[Pd_2Cl_4(\mathbf{3})]\cdot 2.75CH_2Cl_2$.

Bond lengths [Å]		Bond angles [°]	
Pd1–Cl1	2.3019(8)	Cl1–Pd1–Cl2	88.73(3)
Pd1–Cl2	2.319(1)	Cl1–Pd1–S2	83.28(3)
Pd1–N2	2.107(2)	Cl2–Pd1–N2	92.25(6)
Pd1–S2	2.288(1)	N2–Pd1–S21	95.61(6)
Pd2–Cl3	2.329(1)	Cl3–Pd2–Cl4	89.68(3)
Pd2–Cl4	2.3129(9)	Cl3–Pd2–N4	90.35(6)
Pd2–N4	2.111(2)	Cl4–Pd2–S1	84.21(3)
Pd2–S1	2.279(1)	N4–Pd2–S1	96.28(6)

Complexation properties of 6

We had shown in earlier work that the reaction of the previously reported macropentacycle **6** with 1 equiv. of CF_3CO_2H, CF_3SO_3H, or (*S*)-BNPH ((*S*)-1,1′-binaphthyl-2,2′-diyl hydrogenphosphate) gave the salts $[\mathbf{6}H]^+\cdot CF_3CO_2^-$, $[\mathbf{6}H]^+\cdot CF_3SO_3^-$, or $[\mathbf{6}H]^+\cdot BNP^-$, in which the added proton was located on the bridgehead nitrogen atoms in *endo* conformation, being also bound to the three proximal sulfur atoms of the arylthioether groups, as shown by X-ray diffraction analysis.[17] The encapsulated proton was in a neutral [NS3] coordination environment, and the other bridgehead nitrogen atom was in *exo* conformation, which made the molecule unsymmetrical with respect to the plane normal to the $N_{endo}\cdots N_{exo}$ C_3 axis and bisecting the dithioethene bridges. We next wondered if **6** could complex soft metal cations in the same coordination sphere as the proton. Therefore, we tested the ability of **6** to complex Cu^+ and Ag^+. Accordingly, **6** was reacted with either $[Cu(CH_3CN)_4](PF_6)$ or [AgOTs] under inert atmosphere (Scheme 5).

The ^{1}H NMR spectra of the reaction products (Figure 5) were similar to the one observed in the case of the proton adduct in terms of the number of signals and their multiplicities, which indicated that the unsymmetrical structure of the latter was retained in the case of the metal complexes. Therefore the complexes could be formulated $[M(\mathbf{6})]^+$, M=Cu or Ag, which was confirmed by MALDI-TOF analysis (Figures S26–S27). In addition to the oriented nature of the $N_{endo}\cdots N_{exo}$ axis, all three compounds are C_3-chiral, as attested by the equivalence of the three peripheral macrocyclic subunits and the doublets of the isolated methylene groups, this latter point indicating that they are made of pairs of diastereotopic protons. As shown in Figure 5, the positions of the signals changed upon progressing along the series $[\mathbf{6}H]^+$, $[Cu(\mathbf{6})]^+$, $[Ag(\mathbf{6})]^+$: Overall, the signal windows in the aromatic and the aliphatic regions of the spectra shrank upon going from the proton adduct to the silver complex. This is particularly well illustrated by the evolution of the signals of the tosyl methyl (e), the *tert*-butyl, and the δ′ protons, the latter being located in the middle of the chains

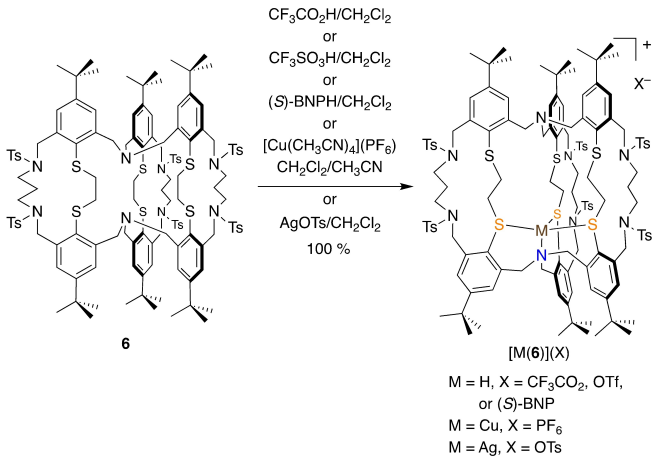

Scheme 5. Reactions of macropentacycle **6** with H^+, Cu^+, and Ag^+ salts.

Research Article
doi.org/10.1002/ejic.202300580

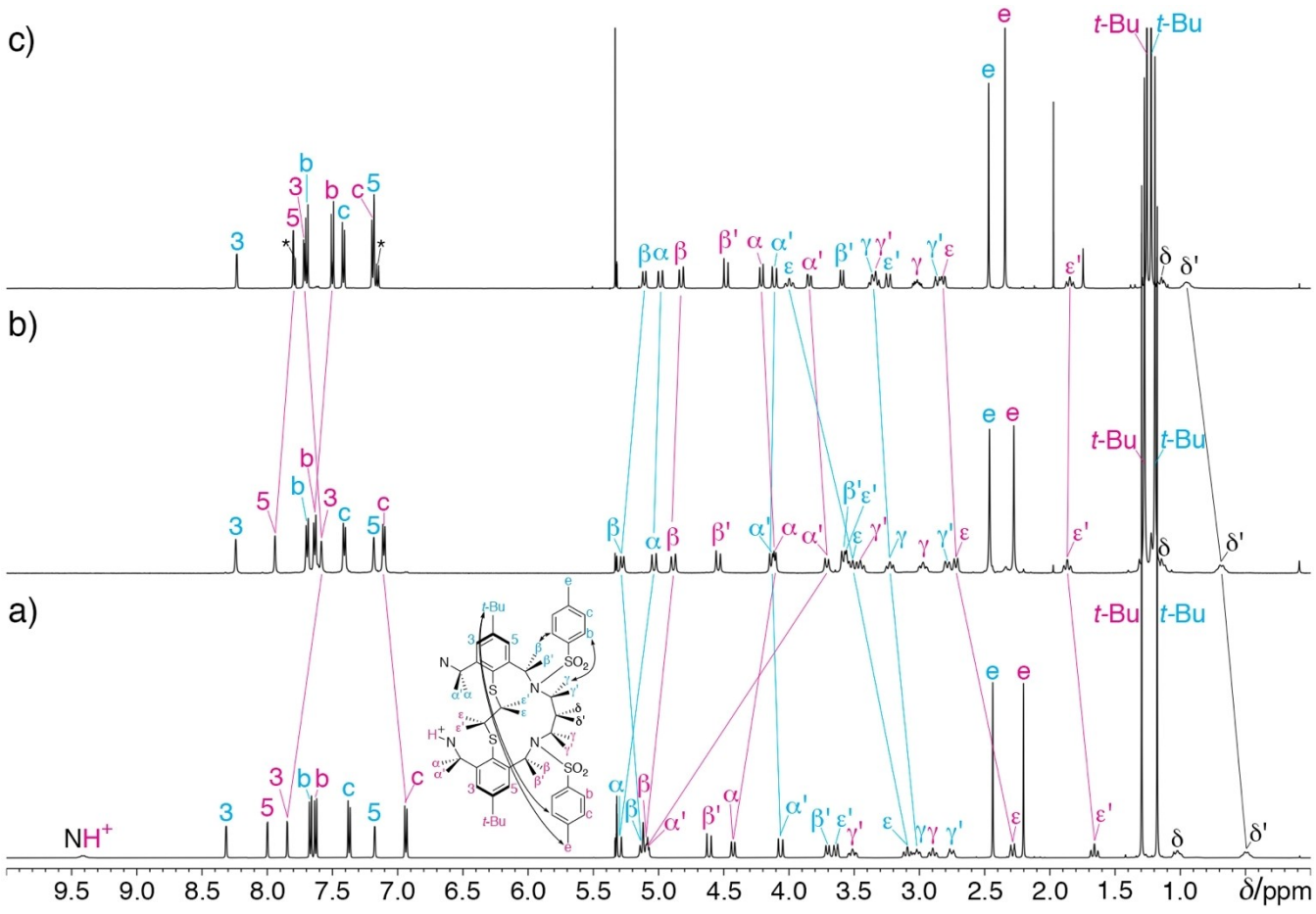

Figure 5. ^{1}H NMR spectra (500 MHz, CD_2Cl_2, 300 K) of (a) [**6**H](CF_3CO_2), (b) [Cu(**6**)](PF_6) and (c) [Ag(**6**)](OTs). The inset show proton labelling, the arrows indicate nOe correlations identified in the case of the proton complex.[14] Color code: magenta for the protons belonging to the *endo* (i) half of [**6**H]$^+$, cyan for those belonging to the *exo* (e) half of [**6**H]$^+$, and black for protons δ and δ′, which are located in the middle. The straight lines indicate the shifts of signals of analogous protons.

connecting the [NS3] tripod subunits. Otherwise, there are signals that undergo a significant shift upon moving from the proton adduct to the copper complex. These signals are those of the protons α_i' (−1.4 ppm), ε_i (+0.4 ppm), and ε_o (+0.4 ppm), and, to a lesser extent, 3_i, c_i, α_o, α_i, β_o, β_i, ε_i', γ_o, and δ′. Significantly, the protons α_i', ε_i, and ε_o are close to the nitrogen and three sulfur atoms that are bound to the cation. The strongest shifts upon going from the Cu^+ to the Ag^+ complex are those of protons ε_o (+0.4 ppm) and δ′ (+0.25 ppm). The chemical shift differences observed upon moving along the series [**6**H]$^+$, [Cu(**6**)]$^+$, and [Ag(**6**)]$^+$ arise from differences in the size of the encapsulated cations *i.e.*, H^+ *vs* Cu^+ (0.96 Å) and Ag^+ (1.26 Å),[18] which can produce different deformations of the macropentacycle.

In the complexes [Cu(**6**)]$^+$ and [Ag(**6**)]$^+$, the metal is encapsulated by an [NS3] tripodal subunit of the type tris(2-(alkylthio)benzylamine). Surprisingly, the coordination chemistry of this kind of ligand has only been reported for Ag^+ in the study of the extraction of silver from an aqueous phase into an organic phase.[19] However, copper complexes of [NS3] tripod ligands of the type $N(CH_2SAr)_3$ with a shorter bond sequence have been reported, as well as their redox properties in the context of the modeling of methionine-rich copper-based metalloenzymes.[20]

Therefore, we studied the redox properties of the copper complex [Cu(**6**)](PF_6) in acetonitrile solution by cyclic voltammetry (Figures S28 and S29) with all potentials referenced to the Fc^+/Fc couple. Between −0.85 and +1.25 V and at a rate of 100 mV s^{-1}, the voltammogram shows two anodic peak potentials, a weak one at 0.16 V, a strong one at 0.89 V, and a weak cathodic peak potential at −0.50 V. When the anodic potential is switched at 0.55 V, that is below 0.89 V, the cathodic peak at −0.50 V is no longer present, which shows that it corresponds to the anodic peak at 0.89 V. The latter could be due to the oxidation of either the unbound *exo* benzylic amine nitrogen atom (0.99 V *vs* SCE reported for tribenzylamine[21]), or the unbound *exo* benzene thioether sulfur atoms (1.02 V *vs.* Fc^+/Fc reported for thioanisole[22]). The cyclic voltammogram of the proton adduct [**6**H]((*S*)-BNP)[17] run under the same conditions (Figures S30–S31) shows a broad anodic peak at *ca.* 0.95 V at 400 mV s^{-1}, but does not show any feature below this potential in the anodic region. This observation indicates that the peak at

Research Article
doi.org/10.1002/ejic.202300580

0.16 V in the cyclic voltammogram of [Cu(**6**)](PF_6) corresponds to the oxidation of Cu^+ to Cu^{2+}, which is irreversible. It is pertinent to compare this redox potential value to those of copper complexes exhibiting similar donor atom environments. The half-wave reduction potential in aqueous solution of the copper(II) complex of the macrocycle [12]aneNS_3, which has the same donor atom set as **6**, was −0.14 V *vs.* Fc^+/Fc;[23] In the case of the Cu(I) complex of the tripod [N_2S_2] ligand *N*,*N*-(2-pyridylmethyl)bis(2-methyl-thiobenzyl)amine in dichloromethane, the $E_{1/2}$ value was 0.23 V *vs.* Fc^+/Fc.[24] Therefore, the oxidation potential of complex [Cu(**6**)]$^+$ is in the expected range.

These data confirm that copper centers in thioether-rich coordination environments are characterized by high redox potentials of the Cu^{2+}/Cu^+ redox couple, hence the significance of the presence of methionine as a ligand in electron transfer metalloproteins, such as blue copper proteins.[25]

Conclusions

Several new strapped derivatives of expanded tetraazatetrathiacalix[4]arenes have been synthesized. The strap is an ethylene bridge connecting two SAr subunits that are in *trans* with respect to each other. It has a twofold synthetic function: (i) functionalization of the aromatic rings with sulfur, (ii) templation of the macrocyclization reactions. This series of macrobicyclic compounds was completed by a macrotricycle and a macropentacycle that were partitioned by the same strap and had been synthesized according to the same principle. The ability of these compounds to act as compartmental macrocyclic ligands was evaluated using soft metal cations such as Pd^{2+}, Cu^+, and Ag^+. Each compartment of the macrobicycle **3** behaved as a single N,S chelate, which coordinated a [$PdCl_2$] complex fragment in square planar geometry as shown by an X-ray crystal structure. In the case of the macropentacycle **6**, as the peripheral nitrogen atoms were protected by tosylation, the coordination of the metal cations was directed into the central macrobicyclic compartment, which could encapsulate Cu^+ and Ag^+ by one of the two [N,3S] tripod chelates, presumably in tetrahedral geometry.

Experimental Section

Materials and methods. Precursor **1** was prepared as described in the literature.[11] Compounds **5** and **6** were available from previous studies.[10d,12] All reagents and solvents were commercial grade and used without further purification. Melting points were determined with an Electrothermal IA9000 series instrument using open glass capillaries and are uncorrected. Elemental analyses were carried out with a VARIO EL elemental analyzer (Elementar Analysensysteme GmbH, Hanau). NMR spectra were recorded on a Bruker 500 MHz Avance III spectrometer. Mass spectra were obtained using the positive ion electrospray ionization modus (ESI) on a Bruker Daltonics ESQUIRE 3000 Plus ITMS or Impact II UHR Qq-TOF instrument. Infrared spectra (4000–400 cm^{-1}) were recorded at 1 cm^{-1} resolution on a Bruker VERTEX 80v spectrometer (equipped with a ATR accessory). MALDI-TOF mass spectra were obtained with a Bruker Daltonix Proflex III spectrometer using dithranol as matrix.

Electrochemical experiments were acquired on a Biologic SP-150 potentiostat. Cyclic voltammetry experiments were performed using a Pt working electrode (0.071 cm^2). The electrode surface was polished routinely with 0.05 μm alumina-water slurry on a felt surface immediately before use. The counter electrode was a Pt coil and the reference electrode was a Ag wire. Samples were prepared in CH_3CN (ACROS organics, anhydrous, 99.8%) using 0.1 mol L^{-1} tetrabutylammonium hexafluorophosphate (*n*-$Bu_4N(PF_6)$, Sigma Aldrich, +99%) as supporting electrolyte.

Compound 2. Solutions of tetraaldehyde **1** (4.71 g, 10.00 mmol) in CH_2Cl_2 (200 mL) and of 1,3-bis(aminomethyl)benzene (2.72 g, 20.00 mmol) in EtOH (200 mL) were added simultaneously, over the course of 4 h to a round-bottom flask containing 600 mL of a 3:1/v:v CH_2Cl_2/EtOH solvent mixture. During addition, the mixture was stirred vigorously and stirring was continued for further 12 h at room temperature after the reagents had been added. After the mixture was concentrated to a final volume of about 300 mL, solid $NaBH_4$ (3.50 g, 92.5 mmol) was carefully added in small portions. The mixture was stirred for further 1 h at room temperature and excess reducing agent quenched by addition of concentrated hydrochloric acid (final pH value ~1). The mixture was evaporated to dryness to give a colorless residue, which was taken up in a mixture of H_2O (200 mL) and CH_2Cl_2 (200 mL). The pH of the aqueous phase was then adjusted to pH 13 utilizing 5 M aqueous KOH solution. The mixture was again stirred for another 1 h. The organic phase was then separated and the aqueous phase was extracted with CH_2Cl_2 (3×30 mL). The combined organic phases were dried with $MgSO_4$, filtered, and evaporated to dryness to give an oily residue. Pure product crystallized from a CH_2Cl_2/EtOH mixture to give 6.20 g (9.10 mmol, 91% yield) of **2** as a colorless, hygroscopic solid. M.p. 272–275 °C. Elemental analysis for $C_{42}H_{45}N_4S_2$ (679.00 g/mol) calcd.: C 74.29, H 8.02, N 8.25%; found: C 73.46, H 8.13, N 8.24%. *m/z* (ESI+, CH_2Cl_2/MeOH): $C_{42}H_{54}N_4S_2$ [M+H$^+$]$^+$ calcd.: 679.4; found: 679.4. ^{1}H NMR (400 MHz, $CDCl_3$) δ [ppm] = 7.42 (s, 2 H, ArH), 7.37 (s, 4 H, ArH), 7.29 (s, 2 H, ArH), 7.21 (s, 4 H, ArH), 3.92 (s, 8 H, $ArCH_2N$), 3.87 (s, 8 H, $ArCH_2N$), 2.66 (s, 4 H, $ArSCH_2$), 1.87 (s, br, 4 H, NH), 1.33 (s, 18 H, $C(CH_3)_3$). ATR IR ν/cm^{-1} = 3424 (m, br), 3312 (m), 3052 (w), 2951 (s), 2920 (s), 2864 (s), 2383 (w), 1595 (m), 1559 (w), 1477 (m), 1446 (s), 1409 (m), 1362 (m), 1339 (m), 1294 (w), 1224 (m), 1200 (m), 1151 (m), 1111 (s), 1099 (s), 985 (w), 970 (w), 927 (w), 904 (m), 881 (m), 817 (m), 775 (s), 745 (s).

Compound 3. The macrobicyclic aza-thiaether **2** (6.20 g, 8.85 mmol) was dissolved in formic acid (30 mL) at 60 °C. Aqueous formaldehyde solution (37%, 30 mL) was added dropwise. The mixture was refluxed for 24 h, evaporated to dryness, and the resulting residue was taken up in H_2O (100 mL) and CH_2Cl_2 (100 mL). The pH value of the aqueous phase was adjusted to 13 using 5 M KOH aqueous solution. The organic phase was then separated and the aqueous phase was extracted with CH_2Cl_2 (3×50 mL). The combined organic phases were dried with $MgSO_4$, filtered, and evaporated to dryness. The crude product was recrystallized from CH_2Cl_2/EtOH to give pure **3** as a colorless solid. Yield: 5.80 g (7.89 mmol, 90%). M.p. 221–223 °C. Elemental analysis for $C_{46}H_{62}N_4S_2$ (735.10 g/mol) calcd.: C 75.15, H 8.50, N 7.60%; found: C 74.83, H 8.26, N 7.64%. *m/z* (ESI+, CH_2Cl_2/MeOH): $C_{46}H_{63}N_4S_2$ [M+H$^+$]$^+$ calcd.: 735.4; found: 735.4. ^{1}H NMR (400 MHz, $CDCl_3$) δ [ppm] = 7.53 (s, 2 H, ArH), 7.35 (s, 4 H, ArH), 7.26 (s, 2 H, ArH), 7.24 (s, 4 H, ArH), 3.68 (s, 8 H, $ArCH_2N$), 3.63 (s, 8 H, $ArCH_2N$), 2.91 (s, 4 H, SCH_2), 2.13 (s, 12 H, NCH_3), 1.33 (s, 18 H, $C(CH_3)_3$). $^{13}C\{^1H\}$-NMR (100 MHz, $CDCl_3$): δ [ppm] = 150.64 ($Ar^CC(CH_3)_3$), 143.48 (Ar^CCH_2), 138.91 (Ar^CCH_2), 131.34 (Ar^CS), 130.85 (Ar^CH), 128.21 (Ar^CH), 128.06 (Ar^CH), 126.71 (Ar^CH), 63.54 ($ArCH_2N$), 60.75 ($ArCH_2N$), 42.21 (NCH_3), 37.18 (SCH_2), 34.62 ($ArC(CH_3)_3$), 31.42 ($C(CH_3)_3$). ATR IR ν/cm^{-1} = 3442

Research Article
doi.org/10.1002/ejic.202300580

(m, br), 3052 (m), 3023 (m), 2963 (s), 2951 (s), 2904 (s), 2867 (s), 2834 (s), 2783 (s), 2757 (s), 2707 (m), 2671 (m), 1596 (m), 1558 (w), 1478 (m), 1456 (s), 1407 (w), 1363 (s), 1340 (m), 1297 (m), 1275 (m), 1257 (m), 1224 (s), 1199 (m), 1178 (m), 1035 (s), 1020 (s), 992 (m), 967 (m), 939 (w), 924 (w), 888 (s), 856 (s), 808 (w), 776 (m), 753 (m), 699 (m), 652 (w), 636 (w), 434 (w).

Compound 4. Solutions of tetraamine **10** (356 mg, 0.75 mmol) in MeOH (15 mL) and of 4-*tert*-butyl-2,6-diformylphenol (325 mg, 1.58 mmol) in CH_2Cl_2 (15 mL) were added simultaneously, over the course of 1 h, to a round-bottom flask containing 60 mL of a 1 : 1/ v : v CH_2Cl_2/EtOH solvent mixture and a catalytic amount of HCOOH. The reaction mixture was stirred at room temperature for 4.5 h. The reaction mixture was cooled to 0 °C, $NaBH_3CN$ (377 mg, 6.00 mmol) was added, and the mixture was stirred overnight at room temperature. The reaction mixture was cooled again to 0 °C, a 2 N aqueous solution of NaOH was added until the gas evolution stopped, and the reaction mixture stirred for another 4 h at room temperature. The solution changed color from yellow to orange in that process. After removal of the solvents under reduced pressure, the residue was dissolved in water and CH_2Cl_2 (50 mL each), and the aqueous phase was extracted with water three times. The combined organic phases were washed three times with 100 mL brine and dried with K_2CO_3. After reducing the volume of the mixture to 50 mL under reduced pressure, 2 N aqueous HCl was added, and the mixture was stirred overnight. After removing the solvent under reduced pressure, the residue was resuspended in CH_2Cl_2 and filtered. The remaining pink solid was dissolved in 50 mL of MeOH and recrystallized from a mixture of MeOH and MeCN. Storage at 4 °C gave the hydrochloride salt of the bicyclic thioether **4** (**4**·4 HCl) in analytic purity in the form of colorless crystals. Yield: 98 mg (0.10 mmol, 13 %). M.p. >250 °C (decomp.). *m/z* (ESI+, CH_3OH) = 823.6 ($C_{100}H_{142}N_8O_4S_4^{2+}$, $[(M+H^+)_2]^{2+}$). ^{1}H-NMR (300 MHz, CD_3OD): δ [ppm] = 7.87 (s, 4 H, ArH), 7.67 (s, 4 H, ArH), 5.02 (d, $^2J_{HH}$ = 12.7 Hz, 4 H, $ArCH_2N$), 4.69 (d, $^2J_{HH}$ = 13.1 Hz, 4 H, $ArCH_2N$), 4.61 (d, $^2J_{HH}$ = 12.7 Hz, 4 H, $ArCH_2N$), 4.39 (d, $^2J_{HH}$ = 13.1 Hz, 4 H, $ArCH_2N$), 2.99 (s, 4 H, SCH_2), 2.13 (s, 12 H, NCH_3), 1.36 (s, 36 H, $C(CH_3)_3$). $^{13}C\{^1H\}$-NMR (100 MHz, DMSO-d_6): δ [ppm] = 152.75 ($Ar^CC(CH_3)_3$), 152.07 ($Ar^CC(CH_3)_3$), 143.40 (Ar^CCH_2), 137.06 (ArCS), 120.34 (ArCH), 45.70 (Ar^CCH_2N), 35.01 ($Ar^CC(CH_3)_3$), 34.13 ($Ar^CC(CH_3)_3$), 31.21 ($C(CH_3)_3$), 30.85 ($C(CH_3)_3$). IR (KBr) ν/cm^{-1} = 3424 (vs, br), 2959 (vs), 2912 (sh), 2869 (sh), 2764 (s, br), 2612 (m, br), 2414 (s, br), 1602 (s), 1583 (sh), 1493 (vs), 1449 (s), 1414 (sh), 1397 (m), 1366 (m), 1300 (w), 1258 (w), 1212 (s), 1160 (w), 1126 (w), 1053 (w), 1007 (w), 926 (w), 892 (w), 851 (w), 755 (w), 738 (w), 586 (w, br), 537 (w, br), 446 (w, br).

Compound 7. A solution of sodium borohydride (1.00 g, 26.0 mmol) in ethanol (160 mL) was carefully added to a solution of tetraaldehyde **1** (2.35 g, 5.0 mmol) in dichloromethane (40 mL) and the resulting reaction mixture was stirred for 17 h at room temperature. The pH was adjusted to less than 7 using 1 N hydrochloric acid and stirred for an additional two hours at room temperature. Subsequently, the solvent was removed under reduced pressure and the resulting residue was suspended in water and dichloromethane (50 mL each). The resulting suspension was filtered, and the isolated solid was washed with water and dichloromethane (10 mL each), and then dried in air, which gave 2.30 g tetraol **7** as a colorless solid. Yield: 4.80 mmol, 96 %. M.p. 191–192 °C. Elemental analysis for $C_{26}H_{38}O_4S_2$ (478.71 g/mol) calcd.: C 65.24, H 8.00, S 13.39 %; found: C 65.26, H 8.06, S 13.28 %. m/z (ESI+, DMSO/CH_3OH): $C_{26}H_{38}NaO_4S_2^+$, $[M+Na^+]^+$ calcd.: 501.3; found: 501.3, $[M+K^+]^+$ calcd.: 517.2; found: 517.2. ^{1}H-NMR (400 MHz, CD_3OD): δ [ppm] = 7.53 (s, 4 H, ArH), 4.80 (s, 8 H, $ArCH_2OH$), 2.74 (s, 4 H, SCH_2), 1.34 (s, 18 H, $ArC(CH_3)_3$). $^{13}C\{^1H\}$-NMR (100 MHz, DMSO-d^6): δ [ppm] = 151.58 ($Ar^CC(CH_3)_3$), 146.27 (Ar^CCH_2OH), 125.66 (Ar^CSCH_2), 123.60 (ArCH), 62.28 (Ar^CCH_2OH), 35.91 (SCH_2), 35.17 ($Ar^CC(CH_3)_3$), 31.76 ($Ar^CC(CH_3)_3$). IR (KBr) ν/cm^{-1} = 3287 (vs, br), 2961 (vs), 2904 (s), 2868 (s), 2652 (w), 1771 (w), 1600 (m), 1561 (w), 1479 (s), 1462 (s), 1440 (sh), 1414 (s), 1363 (s), 1278 (m), 1254 (m), 1241 (sh), 1225 (s), 1202 (s), 1154 (m), 1126 (m), 1063 (vs), 1036 (sh), 1010 (s), 996 (sh), 984 (sh), 917 (w), 891 (sh), 880 (s), 801 (w), 751 (m), 723 (m), 690 (m), 653 (m), 532 (w), 462 (w), 428 (w).

Compound 8. To a solution of the tetraol **7** (2.39 g, 5.00 mmol) in THF (150 mL) was added NEt_3 (4.19 mL, 3.04 g, 30 mmol) and methanesulfonylchloride (2.86 g, 25.0 mmol) to give a colorless suspension, which was stirred for further 12 h at r.t. The solid product was filtered off, washed with H_2O (100 mL) and THF (50 mL), and dried in air to give 3.80 g of the intermediate **8** as a colorless solid. Yield: 4.80 mmol, 96 %. M.p. 177 °C (decomp.). Elemental analysis for $C_{30}H_{46}O_{12}S_6$ (791.1 g/mol) calcd: C 45.55, H 5.86, S 24.32 %; found: C 45.97, H 6.01, S 23.38 %. *m/z* (ESI+, CH_2Cl_2/MeOH): $C_{30}H_{46}O_{12}S_6$ $[M+Na^+]^+$ calcd.: 813.2; found: 813.2. ^{1}H NMR (400 MHz, $CDCl_3$) δ [ppm] = 7.62 (s, 4 H, ArH), 5.52 (s, 8 H, $ArCH_2O$), 3.04 (s, 12 H, OCH_3), 2.90 (s, 4 H, SCH_2), 1.34 (s, 18 H, $C(CH_3)_3$). $^{13}C\{^1H\}$-NMR (100 MHz, CD_2Cl_2): δ [ppm] = 154.25 ($Ar^CC(CH_3)_3$), 139.17 (Ar^CCH_2OS), 131.02 (Ar^CSCH_2), 129.53 (Ar^CCH), 71.15 (CH_2OS), 38.39 (OCH_3), 37.39 (SCH_2), 35.41 ($C(CH_3)_3$), 31.30 ($C(CH_3)_3$). ATR IR ν/cm^{-1} = 3443 (m, br), 3019 (m), 2972 (s), 2938 (s), 2909 (m), 2872 (m), 2509 (w), 2310 (w), 1797 (w), 1634 (sh), 1599 (m), 1480 (m), 1456 (s), 1418 (m), 1343 (vs), 1268 (sh), 1253 (sh), 1231 (s), 1210 (s), 1169 (vs), 1132 (m), 1052 (m), 1037 (sh), 1016 (s), 987 (vs), 968 (vs), 937 (vs), 910 (s), 892 (vs), 847 (vs), 784 (sh), 769 (m), 759 (m), 741 (w), 721 (m), 687 (w), 669 (w), 644 (w), 584 (w), 564 (m), 527 (vs), 514 (s), 485 (m), 464 (w), 443 (w), 430 (w).

Compound 9. (Method A) To a solution of tetraol **7** (1.20 g, 2.50 mmol) in tetrahydrofuran (125 mL) was added solid triphenylphosphine (3.93 g, 15.0 mmol) followed by diisopropylazodicarboxylate (2.95 mL, 15.0 mmol) and diphenylphosphoryl azide (3.24 mL, 15.0 mmol) under ice cooling. The homogeneous reaction mixture was warmed to room temperature and stirred at this temperature for 3 days. A yellow oily residue was obtained by removing all the volatiles under reduced pressure. After purification by column chromatography using an eluent mixture of dichloromethane/*n*-hexane (4 : 1), tetraazide **8** was isolated as 0.5 g of a colorless oil of analytical purity. Yield: 0.84 mmol, 35 %. (Method B). To a solution of compound **8** (1.98 g, 2.50 mmol) in DMF (150 mL) was added NaN_3 (0.71 g, 11.0 mmol), and the resulting mixture was stirred for 2 h. The suspension was combined with 150 mL of ice water to give a colorless solid. The aqueous phase was extracted with CH_2Cl_2 (75 mL) three times. The combined organic phases were washed two times with 200 mL water, then with 200 mL brine and dried with Na_2SO_4. Drying in vacuum provided the product as a colorless oil (1.43 g, 2.47 mmol, 99 %). ^{1}H NMR (400 MHz, $CDCl_3$) δ [ppm] = 7.41 (s, 4 H, ArH), 4.66 (s, 8 H, $ArCH_2$), 2.85 (s, 4 H, SCH_2), 1.34 (s, 18 H, CH_3).). $^{13}C\{^1H\}$-NMR (100 MHz, $CDCl_3$): δ [ppm] = 153.42 ($Ar^CC(CH_3)_3$), 140.67 ($Ar^CCH_2N_3$), 129.52 ($Ar^CSC(CH_3)_3$), 127.23 (Ar^CH), 54.15 ($-CH_2N_3$), 36.58 (SCH_2), 34.94 ($C(CH_3)_3$), 31.20 (($CH_3)_3$).

Compound 10. The tetra azide derivative **8** (1.43 g, 2.47 mmol) was dissolved in 225 mL CH_2Cl_2/MeOH (1 : 2/*v* : *v*). Palladium on coal (10 wt.%, 1.40 g) was added. The reaction mixture was stirred for 15 h under a H_2 atmosphere. The catalyst was separated by filtration and the solvent was removed under reduced pressure. The product was dried in high vacuum and remained as a colorless solid. Yield: 1.15 g (2.43 mmol, 97 %), M.p. 105–110 °C. elemental analysis for $C_{26}H_{42}N_4S_2 \cdot 4H_2O$ (474.77 g/mol) calcd.: C 57.11, H 9.22, N 10.25, S 11.73 %; found: C 56.98, H 7.79, N 9.78, S 10.64 %. *m/z* (ESI+, CH_3OH): $C_{26}H_{43}N_4S_2^+$ $[M+H^+]^+$ calcd.: 475.4; found: 475.4. ^{1}H-NMR (400 MHz, CD_3OD): δ [ppm] = 7.50 (s, 4 H, ArH), 4.10 (s, 8 H, $ArCH_2NH_2$), 2.83 (s, 4 H, SCH_2), 1.37 (s, 18 H, $ArC(CH_3)_3$). $^{13}C\{^1H\}$-NMR (100 MHz, CD_3OD): δ [ppm] = 154.61 ($Ar^CC(CH_3)_3$), 146.02

($Ar^{C}CH_2NH_2$), 129.51 ($Ar^{C}SC(CH_3)_3$), 127.06 (ArCH), 45.32 ($Ar^{C}CH_2NH_2$), 37.41 (SCH_2), 35.83 ($Ar^{C}C(CH_3)_3$), 31.57 ($Ar^{C}C(CH_3)_3$). IR (KBr) ν/cm^{-1} = 3355 (s), 3266 (s), 2955 (vs), 2910 (vs), 2868 (vs), 2626 (s), 2161 (m), 1597 (vs), 1478 (s), 1462 (s), 1411 (m), 1394 (m), 1363 (s), 1289 (w), 1264 (w), 1225 (m), 1203 (m), 1159 (w), 1077 (w), 1045 (w), 979 (m), 885 (vs), 801 (w), 749 (w), 714 (w), 689 (w), 666 (w), 595 (w), 530 (w), 461 (w).

Dinuclear Palladium Complex [Pd_2Cl_4(3)]. To a suspension of the macrobicyclic aza-thioether **3** (147 mg, 0.20 mmol) in acetonitrile (50 mL) was added [$PdCl_2(CH_3CN)_2$] (103.8 mg, 0.40 mmol). The mixture was stirred for 16 h at r.t. to give an orange-colored solid, which was isolated by filtration and recrystallized once from a mixed CH_2Cl_2/EtOH solvent system. Yield: 165 mg (0.15 mmol, 75 %), orange-colored, microcrystalline solid. *m/z* (ESI+, CH_2Cl_2/MeOH): $C_{46}H_{62}Cl_4KN_4Pd_2S_2^+$ $[M+K^+]^+$ calcd.: 1125.2; found 1125.2. ^{1}H-NMR (400 MHz, $CDCl_3$): δ [ppm] = 7.46 (d, $^4J_{HH}$ = 2 Hz, 2 H, ArH), 7.44–7.35 (m, 4 H, ArH), 7.28–7.24 (m, 4 H, ArH), 7.24 (d, $^4J_{HH}$ = 2 Hz, 2 H, ArH), 5.86 (d, $^2J_{HH}$ = 13.2 Hz, 2 H, $ArCH_2N$), 4.13 (d, $^2J_{HH}$ = 13.2 Hz, 2 H, $ArCH_2N$), 3.93 (d, $^2J_{HH}$ = 12.4 Hz, 2 H, $ArCH_2N$), 3.20 (dd, $^2J_{HH}$ = 11.0 Hz, 2 H, $ArCH_2N$), 3.14 (d, $^2J_{HH}$ = 12.4 Hz, 2 H, $ArCH_2N$), 3.03 (d, $^2J_{HH}$ = 13.2 Hz, 2 H, $ArCH_2N$), 2.92 (d, $^2J_{HH}$ = 13.2 Hz, 2 H, $ArCH_2N$), 2.77 (dd, $^2J_{HH}$ = 11.0 Hz, 2 H, $ArCH_2N$), 2.64 (s, 6 H, NCH_3), 2.21 (s, 6 H, NCH_3), 2.00 (s, 4 H, SCH_2), 1.36 (s, 18 H, $C(CH_3)_3$). ^{13}C{^{1}H}-NMR (100 MHz, $CDCl_3$): δ [ppm] = 155.96 ($Ar^{C}C(CH_3)_3$), 142.40 ($Ar^{C}S$), 139.77 ($Ar^{C}CH_2$), 139.30 ($Ar^{C}S$), 133.99 ($Ar^{C}CH_2$), 131.32 ($Ar^{C}H$), 130.80 ($Ar^{C}H$), 130.14 ($Ar^{C}H$), 129.77 ($Ar^{C}H$), 66.73 ($ArCH_2N$), 63.10 ($ArCH_2N$), 49.96 (NCH_3), 43.67 (NCH_3), 38.35 (SCH_2), 35.15 ($C(CH_3)_3$), 31.19 ($C(CH_3)_3$). ATR IR ν/cm^{-1} = 3491 (m, br), 3024 (w), 2964 (s), 2907 (m), 2867 (m), 2846 (m), 2789 (m), 2715 (w), 2234 (w), 1596 (m), 1458 (s), 1417 (m), 1396 (w), 1366 (m), 1299 (w), 1272 (w), 1232 (m), 1198 (m), 1156 (w), 1140 (w), 1124 (w), 1074 (m), 1022 (m), 946 (w), 903 (m), 844 (s), 807 (m), 759 (m), 735 (m), 703 (m), 669 (w), 646 (w), 602 (w), 560 (w), 489 (w), 435 (w). This compound was additionally characterized by X-ray crystallography.

[Cu(6)]PF_6. A solution of [$Cu(CH_3CN)_4$]PF_6 (0.00393 g, 1.0544×10^{-5} mol) in CH_3CN (2 mL) was transferred via canula into a solution of **6** (0.0250 g, 1.0427×10^{-5} mol) in CH_2Cl_2 (4 mL). The colorless reaction mixture was stirred under argon for 3 h. The solvents were evaporated under vacuum. The Schlenk flask containing the product was subsequently handled in a glove box. The colorless solid residue was dissolved into CD_2Cl_2 and transferred into an NMR tube, which was sealed under argon for ^{1}H and ^{13}C NMR analysis. ^{1}H NMR (500.13 MHz, CD_2Cl_2, 300 K): δ [ppm] = 8.240 (s, 3 H; 3_o-H), 7.940 (s, 3 H; 5_i-H), 7.693 (d, $^3J_{HH}$ = 8.1 Hz, 6 H; b_o-H), 7.635 (d, $^3J_{HH}$ = 8.1 Hz, 6 H; b_i-H), 7.584 (s, 3 H; 3_i-H), 7.408 (d, $^3J_{HH}$ = 8.1 Hz, 6 H; c_o-H), 7.182 (s, 3 H; 5_o-H), 7.105 (d, $^3J_{HH}$ = 8.1 Hz, 6 H; c_i-H), 5.267 (d, $^2J_{HH}$ = 11.7 Hz, 3 H; β_o-H), 5.034 (d, $^2J_{HH}$ = 16.6 Hz, 3 H; α_o-H), 4.885 (d, $^2J_{HH}$ = 16.2 Hz, 3 H; β_i-H), 4.541 (d, $^2J_{HH}$ = 16.2 Hz, 3 H; β'_i-H), 4.131 (d, $^2J_{HH}$ = 16.5 Hz, 3 H; α'_o-H), 4.113 (d, $^2J_{HH}$ = 13.1 Hz, 3 H; α_i-H), 3.709 (d, $^2J_{HH}$ = 12.8 Hz, 3 H; α'_i-H), 3.584 (d, $^2J_{HH}$ = 11.6 Hz, 3 H; β'_o-H), 3.577 (d, $^2J_{HH}$ = 18.4 Hz, 3 H; ε'_o-H), 3.524 (d, $^2J_{HH}$ = 13.8 Hz, 3 H; ε_o-H), 3.453 ("t", $^2J_{HH}$ = 13.9 Hz, 3 H; γ'_i-H), 3.226 ("t", $^2J_{HH}$ = 12.8 Hz, 3 H; γ_o-H), 2.972 ("ddd", $^2J_{HH}$ = 16.1 Hz, $^3J_{HH}$ = 11.8 Hz, $^3J_{HH}$ = 4.3 Hz, 3 H; γ_i-H), 2.786 ("d", $^2J_{HH}$ = 14.6 Hz, 3 H; γ'_o-H), 2.719 (d, $^2J_{HH}$ = 13.2 Hz, 3 H; ε_i-H), 2.462 (s, 9 H; e_o-H), 2.275 (s, 9 H; e_i-H), 1.865 ("t", $^2J_{HH}$ = 13.2 Hz, 3 H; ε'_i-H), 1.274 (s, 27 H; *t*-Bu_i-H), 1.193 (s, 27 H; *t*-Bu_o-H), 1.154 (hidden m, 3-H; δ-H), 0.684 ("qd", $^2J_{H,H}$ = 12.1 Hz, 3 H; δ-H); ^{13}C NMR (125.77 MHz, CD_2Cl_2, 300 K): δ [ppm] = 156.0 (4_i-C), 153.7 (4_o-C), 145.0 (d_o-C), 144.3 (d_i-C), 143.3 (2_o-C), 140.8 (6_i-C), 140.2 (6_o-C), 139.0 (a_i-C), 138.0 (2_i-C), 134.0 (3_i-C), 133.9 (a_o-C), 132.1 (1_e-C), 130.6 (c_o-C), 130.4 (c_i-C), 130.0 (5_i-C), 129.2 (5_o-C), 128.9 (1_i-C), 128.3 (b_o-C), 127.6 (b_i-C), 125.0 (3_o-C), 62.1 (α_i-C), 56.7 (α_o-C), 56.0 (β_o-C), 47.6 (β_i-C, γ_i-C, ε_i-C), 47.0 (γ_o-C), 39.6 (ε_o-C), 35.5, 35.2 (*t*-Bu_i(C) and *t*-Bu_o(C)), 31.3, 31.2 (*t*-Bu_i-C and *t*-Bu_o-C), 26.3 (δ-C), 21.9, 21.7 (e_i-C and e_o-C). MALDI-TOF MS (Calibration PEG 1500). Calcd. for $C_{129}H_{162}CuN_8O_{12}S_{12}$ (M^+), 2461.83; found: 2461.87.

[Ag(6)]PF_6. A solution of AgOTs (0.00296 g, 1.0607×10^{-5} mol) in CH_2Cl_2 (2 mL) was transferred via canula into a solution of **6** (0.0250 g, 1.0427×10^{-5} mol) in CH_2Cl_2 (4 mL). The colorless reaction mixture was stirred under argon for 3 h. The solvents were evaporated under vacuum. The Schlenk flask containing the product was subsequently handled in a glove box. The colorless solid residue was dissolved into CD_2Cl_2 and transferred into an NMR tube, which was sealed under argon for ^{1}H and ^{13}C NMR analysis. ^{1}H NMR (500.13 MHz, CD_2Cl_2, 300 K): δ [ppm] = 8.234 (br d, $^4J_{HH}$ = 1.5 Hz, 3 H; 3_o-H), 7.801 (br d, $^4J_{HH}$ = 1.5 Hz, 3 H; 5_i-H), 7.794 (d, $^3J_{HH}$ = 8.5 Hz, 2 H; TsO^--H), 7.154 (d, $^3J_{HH}$ = 8.5 Hz, 2 H; TsO^--H), 7.719 (d, $^4J_{HH}$ = 2.5 Hz, 3 H; 3_i-H), 7.697 (d, $^3J_{HH}$ = 8.5 Hz, 6 H; b_o-H), 7.500 (d, $^3J_{HH}$ = 8.0 Hz, 6 H; b_i-H), 7.416 (d, $^3J_{HH}$ = 8.0 Hz, 6 H; c_o-H), 7.189 (d, $^3J_{HH}$ = 8.0 Hz, 6 H; c_i-H), 7.181 (br d, 3 H; 5_o-H), 5.109 (d, $^2J_{H,H}$ = 12.0 Hz, 3 H; β_o-H), 4.985 (d, $^2J_{HH}$ = 16.0 Hz, 3 H; α_o-H), 4.826 (d, $^2J_{HH}$ = 15.5 Hz, 3 H; β_i-H), 4.483 (d, $^2J_{HH}$ = 15.5 Hz, 3 H; β'_i-H), 4.211 (d, $^2J_{HH}$ = 13.0 Hz, 3 H; α_i-H), 4.112 (d, $^2J_{HH}$ = 16.5 Hz, 3 H; α'_o-H), 3.999 ("ddd", $^2J_{HH}$ = 15.5 Hz, $^3J_{HH}$ = 13.0 Hz, $^3J_{HH}$ = 2.5 Hz, 3 H; ε_o-H), 3.845 (dd, $^3J_{HH}$ = 2.5 Hz, $^3J_{HH}$ = 13.0 Hz, 3 H; α'_i-H), 3.595 (d, $^3J_{HH}$ = 11.5 Hz, 3 H; β'_o-H), 3.361 ("ddd", $^3J_{HH}$ = 10.0 Hz, $^3J_{HH}$ = 12.0 Hz, 3 H; γ_o-H), 3.336 ("t", $^3J_{HH}$ = 12.5 Hz, 3 H; γ'_i-H), 3.239 (d, $^2J_{HH}$ = 15.0 Hz, 3 H; ε'_o-H), 3.016 (m, 3 H; γ_i-H), 2.862 ("ddd", $^2J_{HH}$ = 15.0 Hz, $^3J_{HH}$ = 3.0 Hz, 3 H; γ'_o-H), 2.817 ("ddd", $^2J_{HH}$ = 12.0 Hz, $^3J_{HH}$ = 2.5 Hz, 3 H; ε_i-H), 2.469 (s, 9 H; e_o-H), 2.344 (s, 12 H; e_i-H and TsO^--H), 1.848 ("ddd", $^2J_{HH}$ = 12.0 Hz, $^3J_{HH}$ = 2.0 Hz, 3 H; ε'_i-H), 1.257 (s, 27 H; *t*-Bu_i-H), 1.224 (s, 27 H; *t*-Bu_o-H), 1.145 ("ddd", 3 H; δ-H), 0.953 ("ddd", 3 H; δ-H); ^{13}C NMR (125.77 MHz, CD_2Cl_2, 300 K) : δ [ppm] = 155.4 (4_i-C), 153.2 (4_o-C), 145.1 (d_o-C), 144.2 (d_i-C), 142.3 (2_o-C), 141.7 (2_i-C), 139.3 (6_o-C), 138.7 (a_o-C), 138.6 (6_i-C), 135.0 (3_i-C), 133.8 (a_o-C), 132.6 (1_o-C), 130.8 (5_i-C), 130.6 (c_o-C), 130.3 (c_i-C), 130.2 (5_o-C), 129.4 (1_i-C), 129.0 (TsO^--C), 128.4 (b_o-C), 127.3 (b_i-C), 126.6 (TsO^--C), 125.0 (3_o-C), 60.3 (α_i-C), 58.5 (α_o-C), 55.5 (β_o-C), 47.1, 47.0 (β_i-C, γ_i-C, γ_o-C), 38.0 (ε_o-C), 35.4, 35.2 (*t*-Bu_i(C)-C and *t*-Bu_o(C)-C), 31.3, 31.2 (*t*-Bu_i-C and *t*-Bu_o-C), 27.6 (δ-C), 21.9, 21.7 (e_i-C and e_o-C). MALDI-TOF MS (Calibration PEG 1500). Calcd. for $C_{129}H_{162}AgN_8O_{12}S_{12}$ (M^+), 2505.80; found: 2507.38.

Crystal structure determinations.[26] Suitable single crystals of **2**, **3** and [Pd_2Cl_4(**3**)] were grown by slow evaporation of a DCM/EtOH solvent mixture and mounted on a cryoloop or the tip of a glass fibre using perfluoropolyether oil. The data sets for the compounds **2** and **3** were collected at 180(2) K on a STOE STADIVARI X-ray diffractometer equipped with a GeniX 3D Cu-HF (Xenocx) microfocus X-ray source with a graded multilayer mirror (Cu–Kα, λ = 1.54186 Å) and a hybrid pixel detector Pilatus3 300 K (Dectris). The diffraction experiments for compound [Pd_2Cl_4(**3**)] were carried out at 180 K on a STOE IPDS 2T image plate diffractometer system equipped with a sealed Mo X-ray tube and a graphite monochromator crystal (Mo–Kα, λ = 0.71073 Å). The intensity data were processed with the programs STOE X-AREA software including a numerical absorption correction and in case of compound **2** and **3** a scaling routine.[27] The structures were solved by SHELXT 2018/2[28] using dual methods and refined by full-matrix least-squares techniques on the basis of all data against F^2 using version 2018/3 SHELXL.[29] PLATON was used to search for higher symmetry.[30] All non-hydrogen atoms were refined anisotropically. H atoms were placed in calculated positions and treated isotropically using the 1.2-fold U_{iso} value of the parent atom except methyl protons, which were assigned the 1.5-fold U_{iso} value of the parent C atoms. Unless otherwise noted, all non-hydrogen atoms were refined anisotropically. ORTEP-3 and POV-ray were used for the artwork of the structures.[31]

Crystal Data for 2. $C_{42}H_{54}N_4S_2$, M_r = 679.01 g/mol, orthorhombic space group *Pbca*, *a* = 16.0867(8) Å, *b* = 9.3110(6) Å, *c* = 24.6876(11) Å, *V* = 3697.8(3) Å^3, *Z* = 4, ρ_{calcd} = 1.220 g/cm^3, *T* = 180(2)

Research Article
doi.org/10.1002/ejic.202300580

K, μ(Cu Kα) = 1.562 mm^{-1} (λ = 1.54186 Å), crystal size 0.15×0.14×0.09 mm^3, 19254 reflections measured, 3535 unique, 2283 with $I > 2\sigma(I)$. Final $R_1 = 0.0445$ ($I > 2\sigma(I)$), $wR_2 = 0.1581$ (3535), 260 parameters and 49 restraints, min./max. residual electron density = −0.33/0.22 e/Å^3.

Crystal Data for 3. $C_{46}H_{62}N_4S_2$, M_r = 735.11 g/mol, monoclinic space group $P2_1/c$, a = 13.4069(3) Å, b = 10.6717(2) Å, c = 29.8249(7) Å, V = 4248.74(16) Å^3, Z = 4, ρ_{calcd} = 1.149 g/cm^3, T = 180(2) K, μ(Cu Kα) = 1.394 mm^{-1} (λ = 1.54186 Å), crystal size 0.22×0.18×0.16 mm^3, 34361 reflections measured, 8025 unique, 6542 with $I > 2\sigma(I)$. Final R_1 = 0.0420 ($I > 2\sigma(I)$), wR_2 = 0.1128 (8025), 479 parameters and 0 restraint, min./max. residual electron density = −0.21/0.29 e/Å^3.

Crystal Data for [Pd_2Cl_4(3)]·2.75CH_2Cl_2. $C_{46}H_{62}Cl_4N_4Pd_2S_2$·2.75$CH_2Cl_2$, M_r = 1096.6 + 233.6 g/mol, orthorhombic space group *Pbca*, a = 13.2290(2) Å, b = 19.4723(3) Å, c = 45.9907(11) Å, V = 11847.2(4) Å^3, Z = 8, ρ_{calcd} = 1.484 g/cm^3, T = 180(2) K, μ(Mo Kα) = 1.142 mm^{-1} (λ = 0.71073 Å), crystal size 0.52×0.44×0.36 mm^3, 48805 reflections measured, 14195 unique, 10704 with $I > 2\sigma(I)$. Final R_1 = 0.0383 ($I > 2\sigma(I)$), wR_2 = 0.1177 (14195), 636 parameters and 172 restraints, min./max. residual electron density = −0.99/0.64 e/Å^3.

Acknowledgements

We are particularly grateful to Prof. Dr. E. Hey-Hawkins and Prof. Dr. H. Krautscheid for providing facilities for NMR and X-ray crystallographic measurements. This work was supported by the University of Leipzig and by the Federal Ministry for Education and Research (BMBF) under grant number 02NUK014C. We are also grateful for the German science foundation (DFG) for providing funds for an FTIR spectrometer (Project number 448298270). We thank the embassy of France in Germany for a PROCOPE-MOBILITE 2022 fellowship to JT. We are also grateful to the CNRS, the University of Bourgogne, and the University of Strasbourg for financial support.

Conflict of Interests

The authors declare no conflict of interest.

Data Availability Statement

The data that support the findings of this study are available in the supplementary material of this article.

Keywords: cage compounds · copper · expanded calixarenes · N,S ligands · palladium

[1] C. A. Gibbs, B. P. Fedoretz-Maxwell, J. J. Warren, *Dalton Trans.* **2022**, *51*, 4976–4985.
[2] R. N. V. K. Deepak, B. Chandrakar, R. Sankararamakrishnan, *Biophys. Chem.* **2017**, *224*, 32–39.
[3] J. Liu, S. Chakraborty, P. Hosseinzadeh, Y. Yu, S. Tian, I. Petrik, A. Bhagi, Y. Lu, *Chem. Rev.* **2014**, *114*, 4366–4469.
[4] J. Jiang, I. A. Nadas, M. A. Kim, K. J. Franz, *Inorg. Chem.* **2005**, *44*, 9787–9794.
[5] P. Courville, R. Chaloupka, M. F. M. Cellier, *Biochem. Cell Biol.* **2006**, *84*, 960–978.
[6] A. T. Bozzi, L. B. Bane, W. A. Weihofen, A. L. McCabe, A. Singharoy, C. J. Chipot, K. Schulten, R. Gaudet, *Proc. Natl. Acad. Sci. USA* **2016**, *113*, 10310–10315.
[7] a) J. E. Bulkowski, P. L. Burk, M.-F. Ludmann, J. A. Osborn, *J. Chem. Soc. Chem. Commun.* **1977**, 498–499; b) P. L. Burk, J. A. Osborn, M.-T. Youinou, Y. Agnus, R. Louis, R. Weiss, *J. Am. Chem. Soc.* **1981**, *103*, 1273–1274; c) Y. Agnus, R. Louis, J.-P. Gisselbrecht, R. Weiss, *J. Am. Chem. Soc.* **1984**, *106*, 93–102.
[8] A.-S. Jullien, C. Gateau, C. Lebrun, P. Delangle, *Inorg. Chem.* **2015**, *54*, 2339–2344.
[9] D. S. Warner, C. Limberg, F. J. Oldenburg, B. Braun, *Dalton Trans.* **2015**, *44*, 18378–18385.
[10] a) A. Jeremies, U. Lehmann, S. Gruschinski, F. Schleife, M. Meyer, V. Matulis, O. A. Ivashkevich, M. Handke, K. Stein, B. Kersting, *Inorg. Chem.* **2015**, *54*, 3937–3950; b) A. Jeremies, S. Gruschinski, M. Meyer, V. Matulis, O. A. Ivashkevich, K. Kobalz, B. Kersting, *Inorg. Chem.* **2016**, *55*, 1843–1853; c) A. Jeremies, S. Gruschinski, S. Schmorl, T. Severin, B. Kersting, *New J. Chem.* **2018**, *42*, 7630–7639; d) F. Schleife, C. Bonnot, J.-C. Chambron, M. Börner, B. Kersting, *Chem. Eur. J.* **2022**, *28*, e202104255.
[11] a) B. Kersting, G. Steinfeld, T. Fritz, J. Hausmann, *Eur. J. Inorg. Chem.* **1999**, 2167–2172; b) M. H. Klingele, G. Steinfeld, B. Kersting, *Z. Naturforsch.* **2001**, *56b*, 901–907.
[12] C. Bonnot, J.-C. Chambron, E. Espinosa, R. Graff, *J. Org. Chem.* **2008**, *73*, 868–881.
[13] O. Mitsunobu, *Synthesis* **1981**, *1981*, 1–28.
[14] R. F. Borch, M. D. Bernstein, H. D. Durst, *J. Am. Chem. Soc.* **1971**, *93*, 2897–2904.
[15] S. S. Batsanov, *Acta Crystallogr. Sect. B* **2020**, *B76*, 38–40.
[16] G. Siedle, B. Kersting, *Z. Anorg. Allg. Chem.* **2003**, *629*, 2083–2090.
[17] C. Bonnot, J.-C. Chambron, E. Espinosa, K. Bernauer, U. Scholten, R. Graff, *J. Org. Chem.* **2008**, *73*, 7871–7881.
[18] R. B. Heslop, P. L. Robinson, *Inorganic Chemistry*, **1967**, Elsevier Publishing Company, Amsterdam, London, New-York, p. 726.
[19] Y. Hiruta, T. Watanabe, E. Nakamura, N. Iwasawa, H. Sato, K. Hamada, D. Citterio, K. Suzuki, *RSC Adv.* **2014**, *4*, 9791–9798.
[20] P. R. Martínez-Alanis, B. N. Sánchez Eguía, V. M. Ugalde-Saldívar, I. Regla, P. Demare, G. Aullón, I. Castillo, *Chem. Eur. J.* **2013**, *19*, 6067–6079.
[21] C. K. Mann, *Anal. Chem.* **1964**, *36*, 2424.
[22] K. Taras-Goslinska, M. Jonsson, *J. Phys. Chem. A* **2006**, *110*, 9513.
[23] J. Hormann, O. Verbitsky, X. Zhou, B. Battistella, M. van der Meer, B. Sarkar, C. Zhao, N. Kulak, *Dalton Trans.* **2023**, *52*, 3176–3187.
[24] W. Rammal, H. Jamet, C. Philouze, J.-L. Pierre, E. Saint-Aman, C. Belle, *Inorg. Chim. Acta* **2009**, *362*, 2321–2326.
[25] V. Gómez-Vidales, I. Castillo, *Eur. J. Inorg. Chem.* **2021**, e2021100728.
[26] Deposition Numbers 2295823 (for **2**), 2295824 (for **3**), and 2295825 (for [Pd_2Cl_4(**3**)]) contain the supplementary crystallographic data for this paper. These data are provided free of charge by the joint Cambridge Crystallographic Data Centre and Fachinformationszentrum Karlsruhe Access Structures service.
[27] Stoe & Cie GmbH X-AREA, X-RED32, X-SHAPE and LANA 2019, Stoe & Cie.
[28] G. M. Sheldrick, *Acta Crystallogr. Sect. A* **2014**, *71*, 3–8.
[29] G. M. Sheldrick, *Acta Crystallogr. Sect. C* **2014**, *71*, 3–8.
[30] A. L. Spek, *PLATON - A Multipurpose Crystallographic Tool*; Utrecht University, Utrecht, The Netherlands, **2000**.
[31] L. J. Farrugia, *J. Appl. Crystallogr.* **1997**, *30*, 565.

Manuscript received: September 21, 2023
Revised manuscript received: November 16, 2023
Version of record online: December 21, 2023